




Article

# Development of Fluorescently Labeled SSEA-3, SSEA-4, and Globo-H Glycosphingolipids for Elucidating Molecular Interactions in the Cell Membrane

Sachi Asano <sup>1,2</sup>, Rita Pal <sup>2</sup>, Hide-Nori Tanaka <sup>1,3</sup>, Akihiro Imamura <sup>1,2</sup>, Hideharu Ishida <sup>1,2,3</sup>, Kenichi G. N. Suzuki <sup>1,3,\*</sup> and Hiromune Ando <sup>1,3,\*</sup> 

<sup>1</sup> The United Graduate School of Agricultural Science, Gifu University, 1-1 Yanagido, Gifu 501-1193, Japan; x6103001@edu.gifu-u.ac.jp (S.A.); htanaka@gifu-u.ac.jp (H.-N.T.); aimamura@gifu-u.ac.jp (A.I.); ishida@gifu-u.ac.jp (H.I.)

<sup>2</sup> Department of Applied Bioorganic Chemistry, Gifu University, 1-1 Yanagido, Gifu 501-1193, Japan; rita.ncl@gmail.com

<sup>3</sup> Center for Highly Advanced Integration of Nano and Life Sciences (G-CHAIN), Gifu University, 1-1 Yanagido, Gifu 501-1193, Japan

\* Correspondence: kgsuzuki@gifu-u.ac.jp (K.G.N.S.); hando@gifu-u.ac.jp (H.A.)

Received: 8 November 2019; Accepted: 3 December 2019; Published: 7 December 2019



**Abstract:** Glycosphingolipids (GSLs), such as the globo-series GSLs stage-specific embryonic antigen 3 (SSEA-3), SSEA-4, and Globo-H, are specifically expressed on pluripotent stem cells and cancer cells, and are known to be associated with various biological processes such as cell recognition, cell adhesion, and signal transduction. However, the behavior and biological roles of these GSLs are still unclear. In our previous study, we observed the interactions between the lipid raft and GSLs in real-time using single-molecule imaging, where we successfully synthesized various fluorescent analogs of GSLs (e.g., GM1 and GM3). Here, we have developed fluorescent analogs of SSEA-3, SSEA-4, and Globo-H using chemical synthesis. The biophysical properties of these analogs as raft markers were examined by partitioning giant plasma membrane vesicles from RBL-2H3 cells into detergent-resistant membrane fractions and liquid-ordered/liquid-disordered phases. The results indicated that the analogs were equivalent to native-type GSLs. The analogs could be used to observe the behavior of globo-series GSLs for detailing the structure and biological roles of lipid rafts and GSL-enriched nanodomains during cell differentiation and cell malignancy.

**Keywords:** glycosphingolipid; globo-series; fluorescent analog

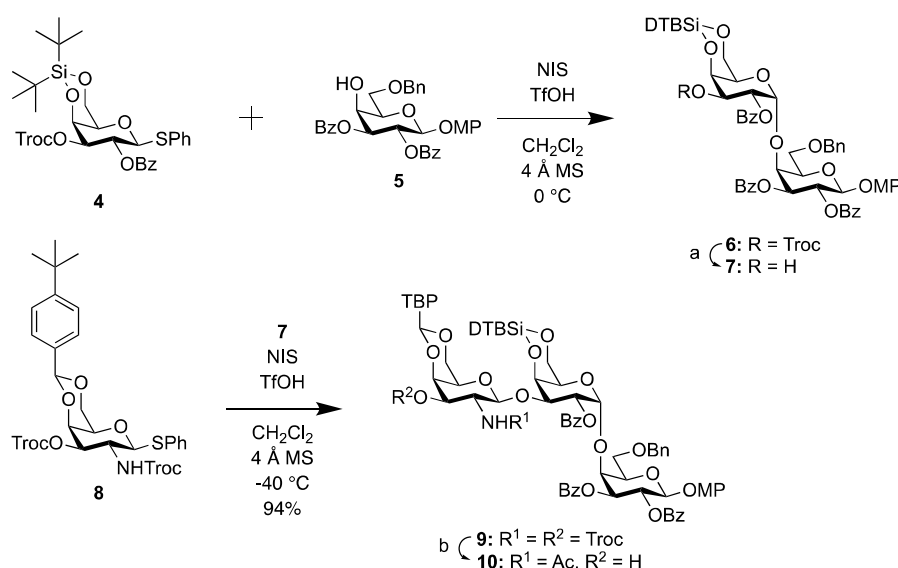
## 1. Introduction

Glycosphingolipids (GSLs) are lipid molecules that are present in the plasma membrane (PM), as well as in cytoplasm and Golgi complex, and contain at least one monosaccharide residue with ceramide lipid that consists of a sphingoid base with a fatty acid amide at the C2 amine [1]. GSLs play significant roles in the PM, such as those in receptors for microbial toxins, mediators of cell adhesion, and modulators of signal transduction [2]. These functions are mediated by cellular microdomains in the PM, such as the lipid raft [3,4] and GSL-enriched microdomains [5]. To detail the distributions, dynamics, and interactions of GSLs with other molecules in the PM, we previously developed chemical methods to synthesize various fluorescent analogs of representative GSLs (e.g., GM1, GM2, GM3, GD1b [6], asialo-GM2, and GalNAc-GD1a [7]) that behave like the native GSLs in the PM. Single-molecule tracking using the fluorescent analogs revealed the specific interactions between GSLs and the lipid raft domain in the PM of living cells [8–10].



### 2.1.2. Synthesis of the Trisaccharide Common Acceptor

The trisaccharide acceptor was synthesized as depicted in Scheme 1. The Gal $\alpha$ (1,4)Gal disaccharide **6** was obtained by di-*tert*-butylsilylene (DTBS)-directed  $\alpha$ -galactosylation [29,30]. In this reaction, the formation of an undesirable orthoester was inevitable due to 2-*O*-Bz of **4**. Although a large amount of trifluoromethanesulfonic acid (TfOH; 0.9 equiv.) could minimize orthoester formation, the orthoester compound was inseparable because it had the same R<sub>f</sub> value as the target disaccharide **6**. The mixture was advanced to cleavage of the 2,2,2-trichloroethoxycarbonyl (Troc) group to produce the disaccharide **7** together with **5** as the hydrolyzed product of the orthoester, which was successfully separated by silica gel column chromatography. For  $\beta$ -galactosaminylation, we employed a 4,6-*O*-*p*-*tert*-butylbenzylidene (TBBzld)-protected GalNTroc donor **8** [31], which was highly soluble in organic solvent, compared to the benzylidenated analog [28]. The trisaccharide **9** was generated by glycosylation in the presence of NIS-TfOH in CH<sub>2</sub>Cl<sub>2</sub> at -40 °C, with an excellent yield (94%). It is of note that the TBBzld-protected donor enabled the large-scale synthesis of the carbohydrate building block, owing to its high solubility. The resulting **9** was converted into the trisaccharide common acceptor **10** for the three target molecules by cleavage of the Troc groups, followed by the selective acetylation of the C2 amino group.



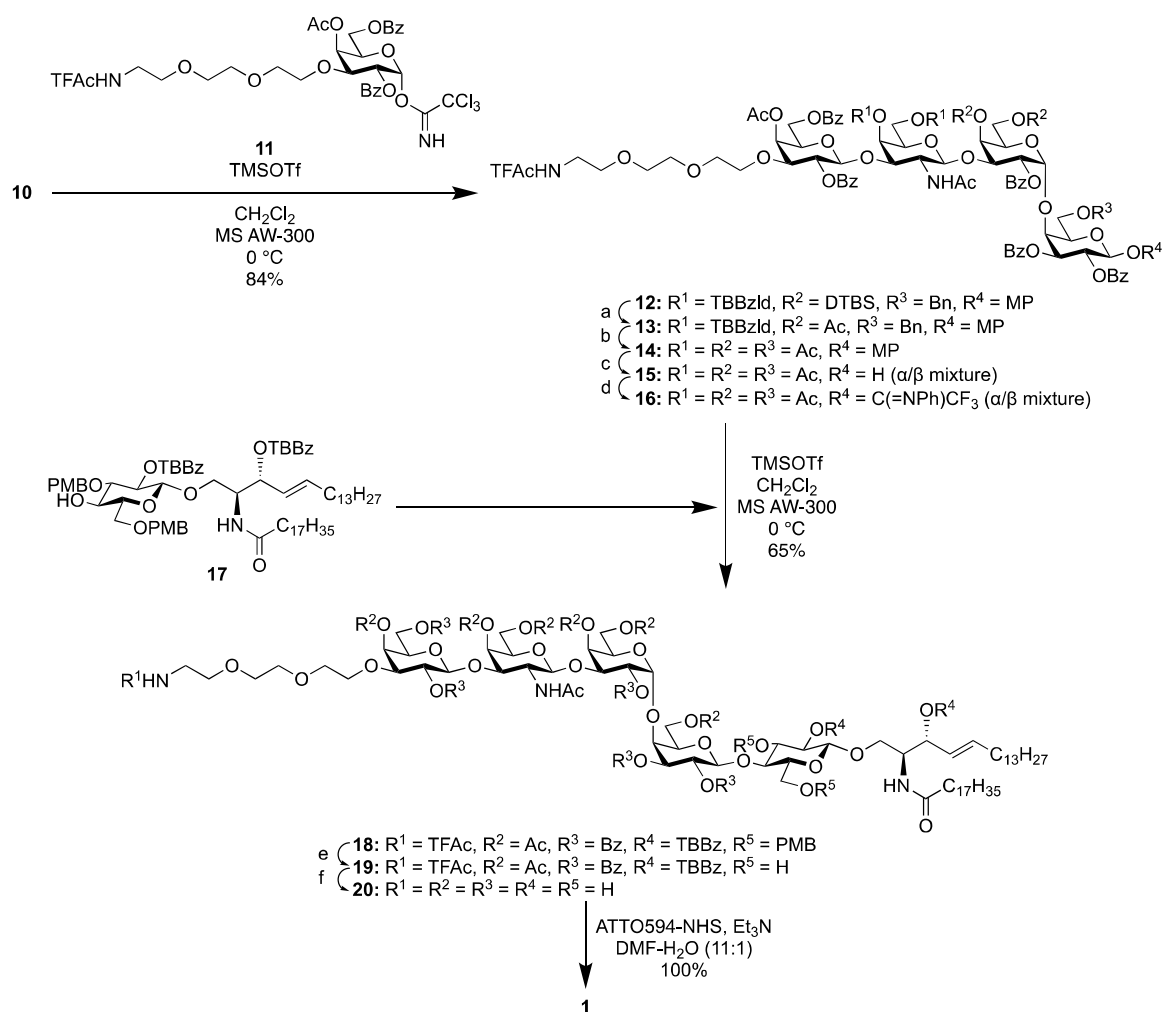
**Scheme 1.** Synthesis of the trisaccharide common acceptor **10**. (a) zinc/AcOH, RT, 78% (2 steps); (b) (i) zinc/ AcOH, RT; (ii) Ac<sub>2</sub>O/ CH<sub>2</sub>Cl<sub>2</sub>, RT, 86% (two steps). Ac = acetyl, Bn = benzyl, Bz = benzoyl, DTBS = di-*tert*-butylsilylene, MP = *p*-methoxyphenyl, MS = molecular sieves, NIS = *N*-iodosuccinimide, TBP = *p*-*tert*-butylphenyl, Tf = trifluoromethanesulfonyl, Troc = 2,2,2-trichloroethoxycarbonyl.

### 2.1.3. Synthesis of the Fluorescent SSEA-3 Probe

For synthesis of the SSEA-3 analog, trisaccharide acceptor **10** was elongated with glycosylation at the 3-OH with a spacer linked to Gal donor **11** to obtain tetrasaccharide **12**, with a yield of 84%. Then, compound **12** was treated with tributylamine hydrofluoride [32] to remove the DTBS group, followed by acetylation, affording compound **13**. The TBBzld and benzyl groups were replaced with acetyl groups to give the fully-acetylated derivative **14**. After cleavage of the MP group, an *N*-phenyltrifluoroacetimidoyl group [33] was introduced at the reducing end, providing tetrasaccharide donor **16**.

To construct the glycolipid framework of SSEA-3, we applied a highly soluble GlcCer acceptor **17** as a coupling partner for the tetrasaccharide donor **16**, which was chemically synthesized by glycosylation of 3-*p*-*tert*-butylbenzoyl (TBBz)-protected Cer acceptor with fully protected Glc donor [31]. In GlcCer **17**, bulky TBBz groups were installed as self-aggregation inhibitors, making **17** highly soluble in organic solvents. This easy-to-handle molecule could overcome the solubility issue of GlcCer, which provided

a yield of 65% for SSEA-3 skeleton **18**. After global deprotection of **18**, ATTO594 dye was conjugated with the terminal amine to provide ATTO594 SSEA-3 **1** (Scheme 2).

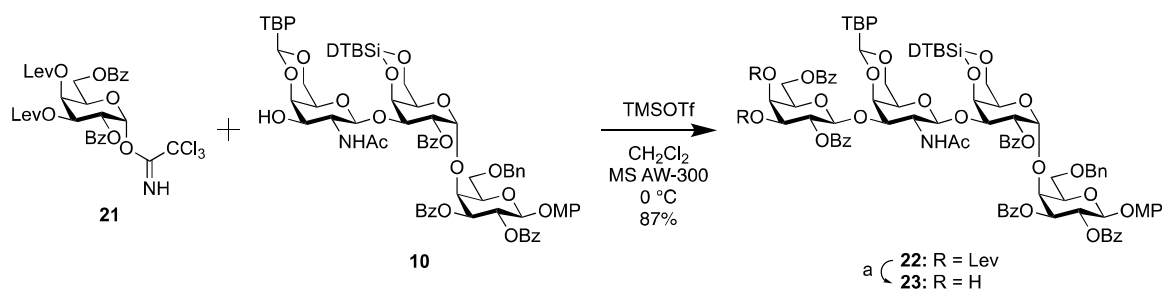


**Scheme 2.** Synthesis of ATTO594 SSEA-3 **1**. (a) (i) TBAHF/ THF, RT; (ii) Ac<sub>2</sub>O, DMAP/ pyridine, RT, 85% (2 steps); (b) (i) H<sub>2</sub> gas, Pd(OH)<sub>2</sub>-C/ dioxane-MeOH (1:1), RT; (ii) Ac<sub>2</sub>O, DMAP/ pyridine, RT, 87% (2 steps); (c) CAN/ MeCN-toluene-H<sub>2</sub>O (6:5:3), 0 °C, 62%; (d) CF<sub>3</sub>C(=NPh)Cl, K<sub>2</sub>CO<sub>3</sub>/acetone, RT, 94%; (e) TFA/ CH<sub>2</sub>Cl<sub>2</sub>, 0 °C, 96%; (f) 1 M NaOH aq./ MeOH-THF (1:1), RT, quant. AW = acid-washed, CAN = cerium (IV) ammonium nitrate, DBU = 1,8-diazabicyclo[5.4.0]undec-7-ene, DMAP = *N,N*-dimethylaminopyridine, DMF = *N,N*-dimethylformamide, NHS = *N*-succinimidyl, PMB = *p*-methoxybenzyl, TBAHF = tributylamine hydrofluoride, TBBz = *p*-*tert*-butylbenzoyl, TBBzld = *p*-*tert*-butylbenzylidene, TFAc = trifluoroacetyl, THF = tetrahydrofuran, TMS = trimethylsilyl.

#### 2.1.4. Synthesis of the Fluorescent SSEA-4 Probe

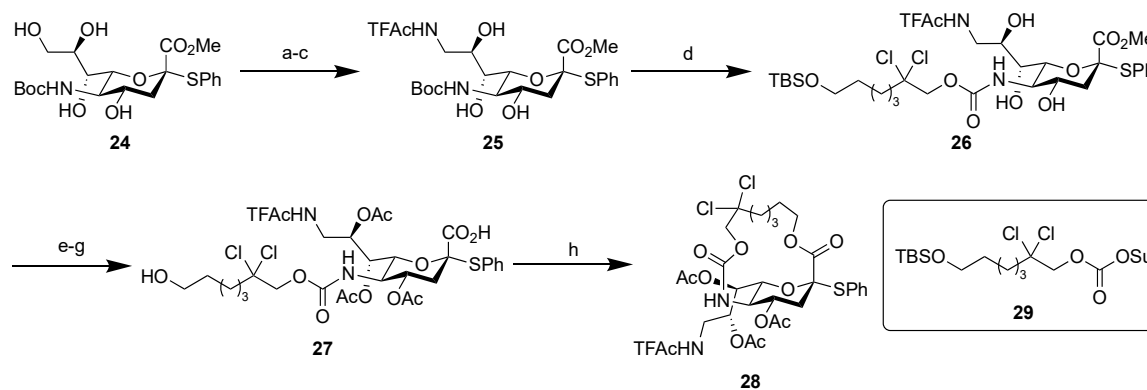
Recently, we developed a method to construct α-sialoside with complete stereoselectivity [34]. In the present study, we exploited this method to construct the glycan moiety of SSEA-4 by sialylation of the SSEA-3 tetrasaccharide.

First, the common trisaccharide acceptor **10** was coupled with the 3,4-*O*-levulinoyl-protected galactosyl donor **21**, affording the tetrasaccharyl derivative **22** with a yield of 87%. Then, the levulinoyl groups were selectively deprotected by treatment with hydrazine acetate in MeOH-tetrahydrofuran (THF), affording the tetrasaccharyl diol acceptor **23** (Scheme 3).



**Scheme 3.** Synthesis of the tetrasaccharyl acceptor **23**. (a) hydrazine acetate/ MeOH-THF (1:5), RT, 95%. Lev = levulinoyl.

Next, the sialyl donor was prepared as shown in Scheme 4. To conjugate fluorescent dye with C9 amino group at the final step, we needed to convert C9 hydroxyl group into a trifluoroacetyl-protected amino group in advance. We chose a *tert*-butoxycarbonyl (Boc) group as a protective group of the C5 amino group to retain the C9-trifluoroacetamido group during the retrieval of the C5 amino group. The Boc group was also expected to be insusceptible to the reaction conditions for replacing the C9 hydroxyl group with a trifluoroacetamido group. First, the C9 hydroxyl group in the *N*-Boc sialic acid derivative **24** [35] was protected with a Ts group, followed by azidation and one-pot reduction of the azido group and trifluoroacetylation of the resulting amine, producing the C9-trifluoroacetamido derivative **25**. Then, the Boc group was cleaved by treatment with trifluoroacetic acid, and the resulting amine was condensed with the *N*-succinimidyl carbonate **29**, which was prepared from alcohol **S8** (see Supporting Information) in situ, giving the carbamate derivative **26**. After acetylation of C4, 7, and 8 hydroxyl groups, demethylation, and cleavage of the TBS group, we performed intramolecular cyclization of compound **27** under the Mitsunobu condition to obtain the sialyl donor **28** without any intermolecular condensation. The use of bis(2-methoxyethyl) azodicarboxylate (DMEAD) [36,37] facilitated the separation of **28** from the hydrazine derivative produced from DMEAD due to its solubility in water.

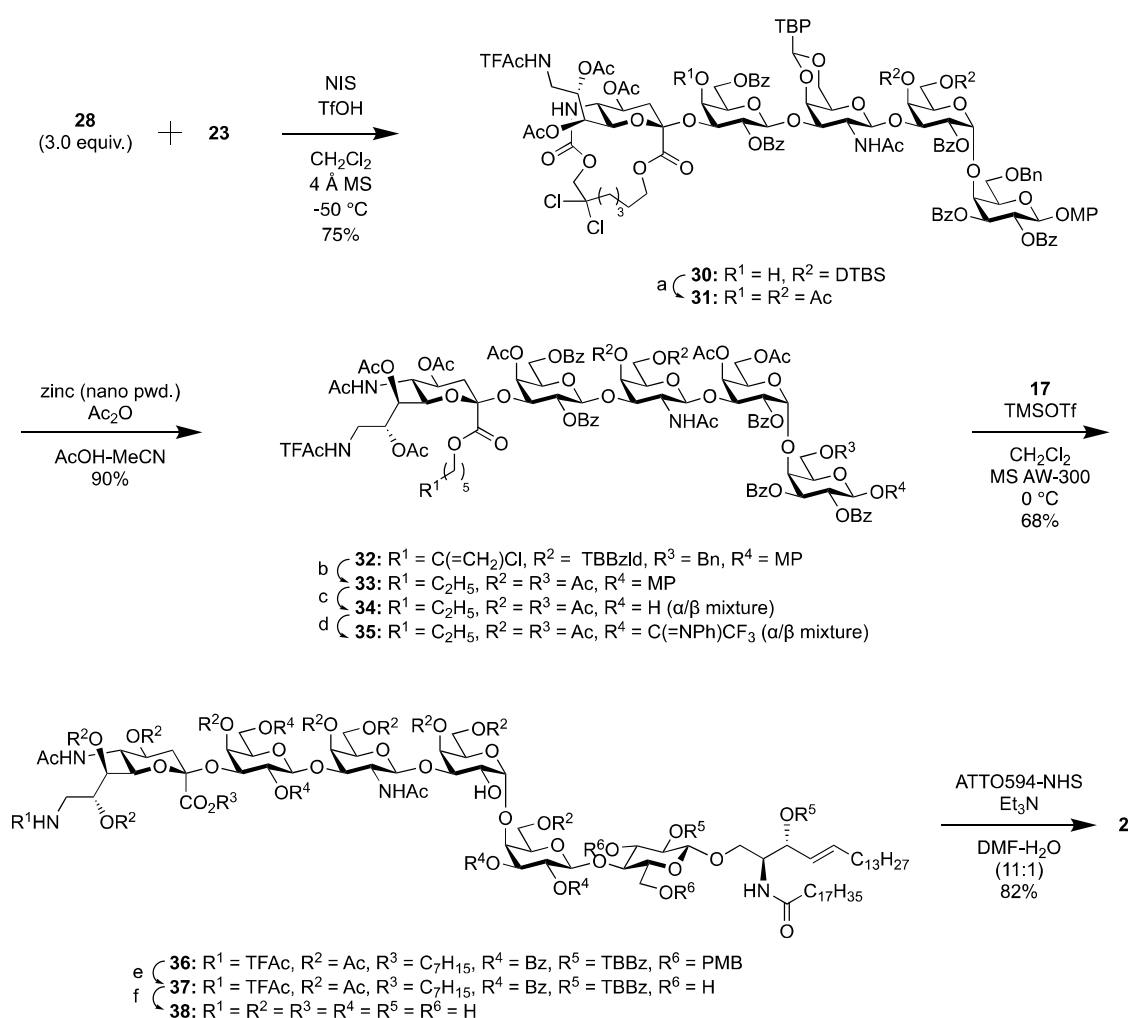


**Scheme 4.** Synthesis of the sialyl donor **28**. (a) TsCl/ CH<sub>2</sub>Cl<sub>2</sub>-pyridine (1:1), 0 °C, 88%; (b) NaN<sub>3</sub>, 18-crown-6/ DMF, Drierite, 80 °C, 92%; (c) H<sub>2</sub> gas, Pd(OH)<sub>2</sub>-C, TFAcOMe, Et<sub>3</sub>N/ MeOH, RT, 95%; (d) (i) TFA, anisole/ CH<sub>2</sub>Cl<sub>2</sub>, 0 °C; (ii) **29**/ MeCN-MeOH (1:1), RT, 84% (2 steps); (e) Ac<sub>2</sub>O, DMAP/ pyridine, RT, 92%; (f) LiI/ pyridine, 100 °C, 94%; (g) TBAF, AcOH/ THF, RT, 87%; (h) PPh<sub>3</sub>, DMEAD/ THF, RT, 91%. Boc = *tert*-butoxycarbonyl, DMEAD = bis(2-methoxyethyl) azodicarboxylate, Su = *N*-succinimidyl, TBAF = tetra-*n*-butylammonium fluoride, TBS = *tert*-butyldimethylsilyl, Ts = *p*-toluenesulfonyl.

Previously, we chemically synthesized various gangliosides and their analogs containing one or more sialic acid units. However, direct approaches to introduce sialic acid units to an oligosaccharide moiety have been avoided due to the uncertainties of stereoselectivity during sialylation. Here, we tried to introduce a sialic acid unit directly to the oligosaccharide using the fully  $\alpha$ -selective sialylation method developed by our group. Although 3.0 equiv. of donor **28** was used to complete the reaction

because of the self-decomposition of **28**, we coupled **28** with the tetrasaccharyl acceptor **23** at  $-50\text{ }^{\circ}\text{C}$ , with a yield of 75%. After the removal of the DTBS group [32], we examined the opening of the 16-membered ring in the pentasaccharide **31**. By following the reported procedure [34], compound **31** was treated with zinc powder in acetic acid. However, the reaction proceeded very slowly, which is probably due to the poor solubility of the reactant. When we diluted the reaction mixture with acetonitrile, the reaction proceeded more quickly but gradually produced an *N*-acetyl-8-hydroxy derivative resulting from O to N acetyl migration [38]. To obtain a single product, compound **31** was treated with zinc powder and an excess amount of acetic anhydride in AcOH-MeCN, successfully delivering **32** at a high yield. Compound **32** was advanced to hydrogenolysis, acetylation of the hydroxyl groups, cleavage of the MP group, and *N*-phenyltrifluoroacetimidoylation to provide the pentasaccharyl donor **35**.

Donor **35** was elongated with the GlcCer acceptor **17**, as mentioned above for the synthesis of fluorescent SSEA-3, producing the SSEA-4 glycolipid framework **36**, with a yield of 68%. Global deprotection and the introduction of the ATTO594 dye delivered the target ATTO594 SSEA-4 **2** (Scheme 5).



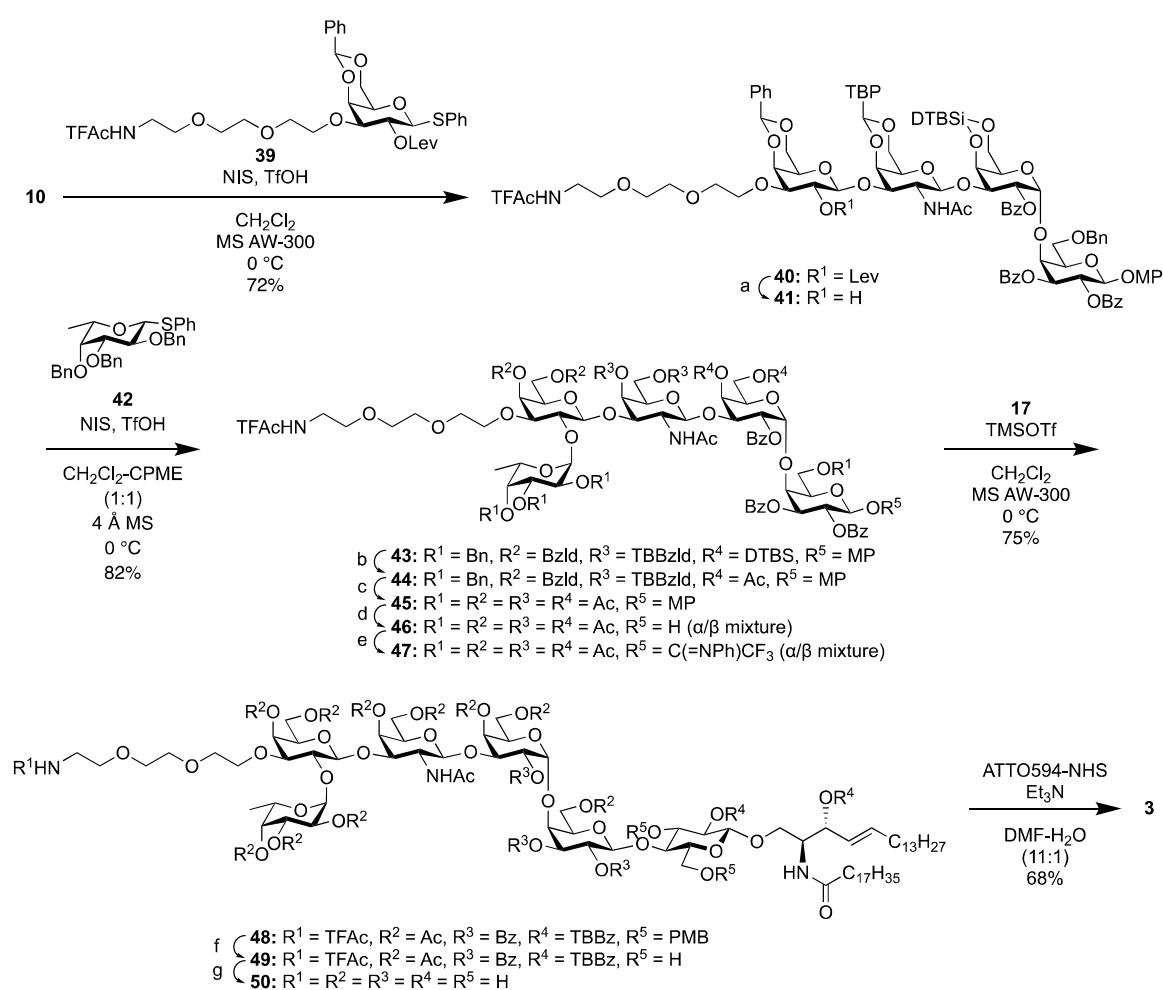
**Scheme 5.** Synthesis of ATTO594 SSEA-4 **2**. (a) (i) TBAHF/ THF, RT; (ii) Ac<sub>2</sub>O, DMAP/ pyridine, RT, 97% (2 steps); (b) (i) H<sub>2</sub> gas, Pd(OH)<sub>2</sub>-C/ dioxane-MeOH (1:1), RT; (ii) Ac<sub>2</sub>O, DMAP/ pyridine, RT, 82% (2 steps); (c) CAN/ MeCN-toluene-H<sub>2</sub>O (6.5:3), 0 °C, 65%; (d) CF<sub>3</sub>C(=NPh) Cl, K<sub>2</sub>CO<sub>3</sub>/ acetone, RT, 94%; (e) TFA/ CH<sub>2</sub>Cl<sub>2</sub>, 0 °C, 96%; (f) 1 M NaOH aq./ MeOH-THF (1:1), RT, 92%.



## 2.1.5. Synthesis of the Fluorescent Globo-H Probe

First, the tetrasaccharyl acceptor **41** was prepared. The galactosyl donor **39**, protected with a levulinoyl group at the C2 hydroxyl group, was coupled with the trisaccharyl common acceptor **10** to yield the  $\beta$ -galactoside **40**. In this case, acid-washed 4 Å molecular sieves were used to suppress the formation of an orthoester. Next, cleavage of the levulinoyl group was achieved selectively to obtain the tetrasaccharyl acceptor **41**, with a high yield of 94%.

For furnishing  $\alpha$ -fucoside, we used the synergic solvent effect of cyclopentyl methyl ether and  $\text{CH}_2\text{Cl}_2$  [39]. The Fuc donor **42** [40] was coupled with the tetrasaccharyl acceptor **41** at 0 °C, building **43** with a yield of 82% as a single  $\alpha$ -anomer. After manipulation of the protecting groups, the obtained donor **47** was elongated with the GlcCer acceptor **17**, giving the Globo-H framework **48**, with a yield of 75%. Global deprotection and the introduction of the ATTO594 dye delivered the target ATTO594 Globo-H **3** (Scheme 6).



**Scheme 6.** Synthesis of ATTO594 Globo-H **3**. (a) hydrazine acetate/ MeOH-THF (1:5), RT, 94%; (b) (i) TBAHF/ THF, RT; (ii) Ac<sub>2</sub>O, DMAP/ pyridine, RT, 93% (2 steps); (c) (i) H<sub>2</sub> gas, Pd(OH)<sub>2</sub>-C/dioxane-MeOH (1:1), RT; (ii) Ac<sub>2</sub>O, DMAP/ pyridine, RT, 88% (2 steps); d) CAN/ MeCN-toluene-H<sub>2</sub>O (6:5:3), 0 °C, 65%; (e) CF<sub>3</sub>C(=NPh) Cl, K<sub>2</sub>CO<sub>3</sub>/acetone, RT, 95%; (f) TFA/ CH<sub>2</sub>Cl<sub>2</sub>, 0 °C, 97%; g) 1 M NaOH aq./ MeOH-THF (1:1), RT, 98%. CPME = cyclopentyl methyl ether.

## 2.2. Biophysical and Biochemical Evaluation

### 2.2.1. Cold-Triton Solubility of the Fluorescent Probes in the PM

Putative raft-associated molecules are insoluble in detergent-resistant membrane (DRM) fractions [41]. Here, the cold-Triton solubilities of the chemically synthesized fluorescent probes in T24 human epithelial cells were examined by following the procedure we reported previously [8]. The cells in which the fluorescent probes were incorporated were treated with cold Triton X-100 and observed by epifluorescence microscopy (Figure 2). All of the synthesized analogs remained in the PM (=DRM), indicating that they retained their properties.

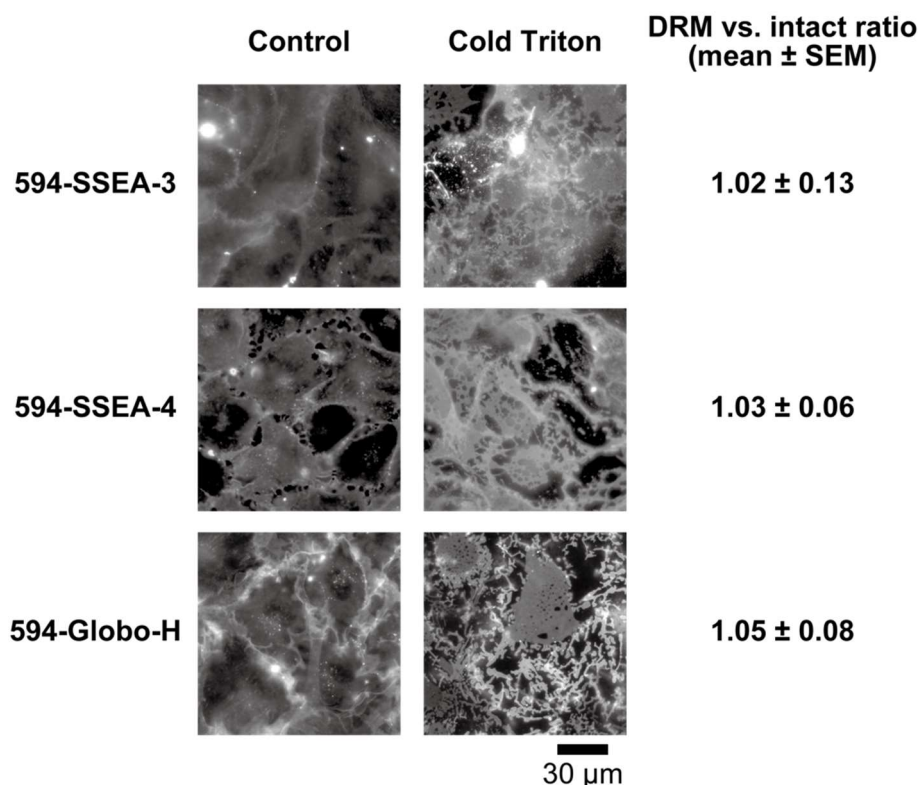


**Figure 2.** Cold-Triton solubility of the fluorescent analogs. The number of cells examined for each probe was >18.

### 2.2.2. Partitioning of the Fluorescent Probes between the Lo/Ld Phases

We examined the partitioning of the fluorescent analogs by using giant PM vesicles (GPMVs), which are largely depleted of the actin-based membrane skeleton, but are considered to contain the full complement of lipids and proteins of the native PM, separating them into the liquid-ordered (Lo, the putative raft phase) and liquid-disordered (Ld) phases [42–44]. Upon cooling the GPMVs, separation of the Lo and Ld phases could be observed (Figure 3).



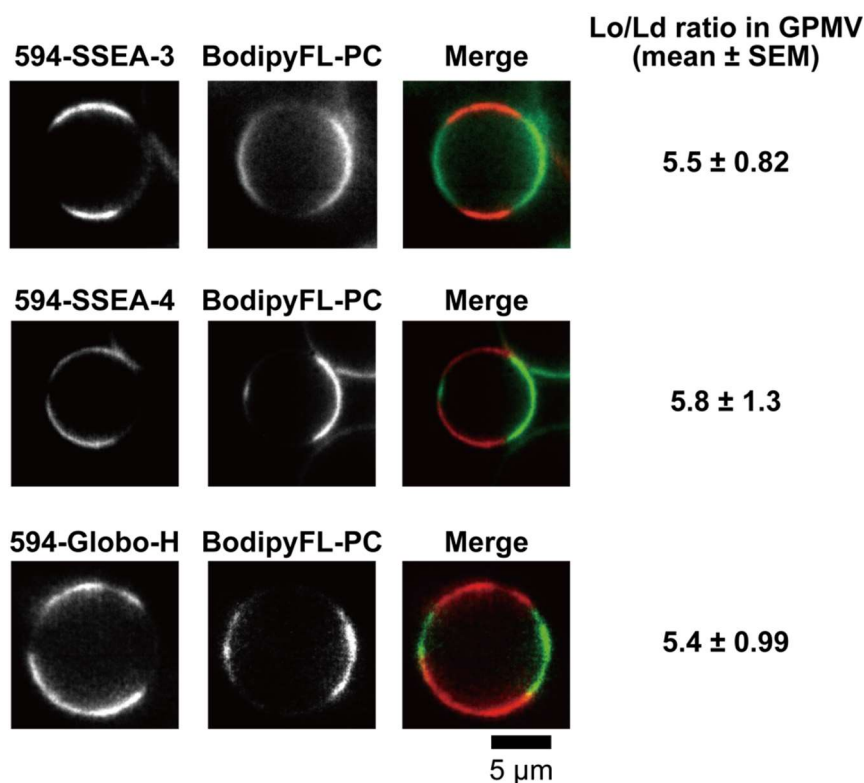


**Figure 3.** Partitioning of the fluorescent analogs into the Lo- and Ld-like domains in giant PM vesicles (GPMVs) of RBL-2H3 cells at 10 °C. Still images taken from simultaneous two-color video sequences. The number of GPMVs examined for each probe was >14.

GPMVs were prepared from RBL-2H3 cells at 10 °C, in which each of the fluorescent analogs and BodipyFL-PC, as Ld-like domain markers, were pre-incorporated. All of the synthesized analogs were preferentially partitioned into the Lo phase, indicating that they all retained their raftophilic properties.

### 3. Materials and Methods

#### 3.1. Chemical Section

Detailed synthetic procedures and NMR spectra for all new compounds are described in the Supplementary Materials.

#### 3.2. Biological Evaluations

We carried out two biological evaluations following the reported procedures [8].

##### 3.2.1. Evaluation of Cold-Triton Solubility

For the epi-fluorescence imaging of fluorescent GSL analogs incorporated in the PM, the analogs were first dispersed in P-HBSS at a final concentration of 1.0 µM, and the dispersed solution was incubated with T24-cell PM at 22 °C for 15 min. Then, the cells were chilled on ice-water (2.8 °C), washed three times with pre-chilled P-HBSS, and incubated in pre-chilled P-HBSS containing 1% (v/v) Triton X-100 on ice-water for 15 min [41]. The Triton-treated cells were washed three times with cold P-HBSS, washed twice with pre-chilled PBS, fixed with 4% paraformaldehyde in PBS for 90 min, and observed under a Nikon Ts-2FL epi-fluorescence microscope equipped with a CMOS camera (DS-Qi2).

### 3.2.2. Formation and Microscopic Observation of GPMVs

RBL-2H3 cells grown on a glass-bottom dish (Iwaki) were washed twice with P-HBSS (without phenol red and sodium bicarbonate; Nissui) and buffered at pH 7.4 with 2 mM PIPES. For the incorporation of the fluorescent ganglioside analogs into the PM, first, a 1- $\mu$ L aliquot of the methanol stock solution of a fluorescent lipid analog (1 mM) was dried to make a thin film on the bottom of a vial and 100  $\mu$ L P-HBSS was added. After vigorous vortexing for 1 min, the mixture was sonicated for 5 min. Subsequently, 0.1 mL of this suspension (final analog concentration of 10  $\mu$ M) was overlaid on the cells in each glass-bottom dish, followed by incubation at 22 °C for 12 min. To mark the Ld-like domains, BodipyFL-PC was incorporated in the PM. To mark the Lo-like domains in GPMVs, the cells were incubated in 10  $\mu$ M ATTO594-SSEA-3, ATTO594-SSEA-4, or ATTO594-Globo-H at 22 °C for 12 min.

After washing the cells three times with P-HBSS, membrane blebbing was induced by incubating the cells in 25 mM formaldehyde and 2 mM dithiothreitol in P-HBSS at 37 °C for 1 h. During this incubation period, numerous blebs were generated and detached from the cells to form GPMVs. The dish was moved onto the microscope stage of a TIRF microscope, based on an Olympus IX83, incubated at 20 °C for 15 min to let the GPMVs settle on the glass bottom, and cooled by circulating a chilled water-ethanol solution (−5 °C) so that the temperature of the top surface of the glass (facing the P-HBSS solution) stabilized at 10 °C. Under these conditions, the majority (>90%) of the GPMVs exhibited two coexisting domains: Ld-like domains preferentially concentrating BodipyFL-PC and Lo-like domains preferentially concentrating the GSL probe, as simultaneously observed by oblique angle illumination with 488 and 594-nm laser beams in our TIRF microscope. The focus was adjusted to collect the fluorescence signal emitted from the equatorial phase of the blebs. Images were recorded simultaneously in two emission channels (520 and 630 nm, or 520 and 670 nm) at a rate of 30 Hz. To estimate the partition coefficients of the various GSL analogs, only the first or second frame of the movie was used, which also minimized the photobleaching effect.

## 4. Conclusions

We have achieved the synthesis of fluorescent analogs of SSEA-3, SSEA-4, and Globo-H, which all retained the biophysical properties as raft molecules in the PM. To construct the trisaccharyl acceptor **10** and GSL frameworks **18**, **36**, and **48**, we applied *p*-*tert*-butyl-substituted protective groups (TBBzd and TBBz) for the first time toward the chemical synthesis of the complex glycoconjugates. For the synthesis of the SSEA-4 analog, we also achieved the direct sialylation of the SSEA-3 tetrasaccharide moiety, which enabled the synthesis of various biofunctionalized molecules, including sialic acid(s).

Given the high pluripotency of hESCs and hiPSCs, and the high proliferation capacity of cancer cell tissues, it has been difficult to understand the behavior of these molecules in the PM of these cells. The fluorescent probes we have developed in this study will accelerate the study of microdomains during cell differentiation and cell malignancy.

**Supplementary Materials:** Supplementary materials can be found at <http://www.mdpi.com/1422-0067/20/24/6187/s1>.

**Author Contributions:** Conceptualization, K.G.N.S. and H.A.; methodology, S.A, R.P, H.-N.T., A.I., K.G.N.S., and H.A.; investigation, S.A., R.P. and K.G.N.S.; data curation, S.A, R.P., K.G.N.S., and H.A.; writing—original draft preparation, S.A., K.G.N.S., and H.A.; writing—review and editing, H.-N.T., A.I., H.I., K.G.N.S., and H.A.; visualization, S.A.; supervision, K.G.N.S. and H.A.; project administration, H.I. and H.A.; funding acquisition, H.I., K.G.N.S., and H.A.

**Funding:** This work was supported in part by JSPS KAKENHI Grant Numbers JP19J10858 (S.A.), JP15K07409 (H.I.), JP18K05461 (H.-N.T.), JP18H02401 (K.G.N.S.), JP18H04671 (K.G.N.S.), JP15H04495 (H.A.), and JP18H03942 (H.A.); JST CREST Grant Number JPMJCR18H2 (K.G.N.S. and H.A.); and by the Mizutani Foundation for Glycoscience (K.G.N.S. and H.A.).

**Conflicts of Interest:** The authors declare no conflict of interest. The funders had no role in the design of the study; in the collection, analyses, or interpretation of data; in the writing of the manuscript; or in the decision to publish the results.

## Abbreviations

|     |                     |
|-----|---------------------|
| Cer | Ceramide            |
| Fuc | Fucose              |
| Gal | Galactose           |
| Glc | Glucose             |
| Neu | Neuraminic acid     |
| PC  | Phosphatidylcholine |

## References

1. Schnaar, R.L.; Kinoshita, T. Glycosphingolipids. In *Essentials of Glycobiology*, 3rd ed.; Varki, A., Cummings, R.D., Esko, J.D., Stanley, R., Hart, G.W., Aebi, M., Darvill, A.G., Kinoshita, T., Packer, N.H., Prestegard, J.H., et al., Eds.; Cold Spring Harbor: New York, NY, USA, 2015–2017; Chapter 11.
2. Lingwood, C.A. Glycosphingolipid functions. *Cold Spring Harb. Perspect. Biol.* **2011**, *3*, a004788. [[CrossRef](#)] [[PubMed](#)]
3. Simons, K.; Ikonen, E. Functional rafts in cell membranes. *Nature* **1997**, *387*, 569–572. [[CrossRef](#)] [[PubMed](#)]
4. Simons, K.; Gerl, M.J. Revitalizing membrane rafts: New tools and insights. *Nat. Rev. Mol. Cell Biol.* **2010**, *11*, 688–699. [[CrossRef](#)] [[PubMed](#)]
5. Hakomori, S. Cell adhesion/recognition and signal transduction through glycosphingolipid microdomains. *Glycoconj. J.* **2000**, *17*, 143–151. [[CrossRef](#)] [[PubMed](#)]
6. Komura, N.; Suzuki, K.G.N.; Ando, H.; Konishi, M.; Imamura, A.; Ishida, H.; Kusumi, A.; Kiso, M. Syntheses of fluorescent gangliosides for the studies of raft domains. *Methods Enzymol.* **2017**, *597*, 239–263. [[PubMed](#)]
7. Koikeda, M.; Komura, N.; Tanaka, H.-N.; Imamura, A.; Ishida, H.; Kiso, M.; Ando, H. Synthesis of ganglioside analogs containing fluorescently labeled GalNAc for single-molecule imaging. *J. Carbohydr. Chem.* **2019**, *38*, 509–527. [[CrossRef](#)]
8. Komura, N.; Suzuki, K.G.N.; Ando, H.; Konishi, M.; Koikeda, M.; Imamura, A.; Chadda, R.; Fujiwara, T.K.; Tsuboi, H.; Sheng, R.; et al. Raft-based interactions of gangliosides with a GPI-anchored receptor. *Nat. Chem. Biol.* **2016**, *12*, 402–410. [[CrossRef](#)]
9. Suzuki, K.G.N.; Ando, H.; Komura, N.; Fujiwara, T.K.; Kiso, M.; Kusumi, A. Development of new ganglioside probes and unraveling of raft domain structure by single-molecule imaging. *Biochim. Biophys. Acta* **2017**, *1861*, 2494–2506. [[CrossRef](#)]
10. Suzuki, K.G.N.; Ando, H.; Komura, N.; Fujiwara, T.; Kiso, M.; Kusumi, A. Unraveling of lipid raft organization in cell plasma membranes by single-molecule imaging of ganglioside probes. *Adv. Exp. Med. Biol.* **2018**, *1104*, 41–58.
11. Hakomori, S.; Siddiqui, B.; Li, Y.-T.; Li, S.-C.; Hellerqvist, C.G. Anomeric structures of “globoside” and ceramide trihexoside of human erythrocytes and “BHK” fibroblasts. *J. Biol. Chem.* **1971**, *246*, 2271–2277.
12. Hakomori, S. Structure and function of glycosphingolipids and sphingolipids: Recollections and future trends. *Biochim. Biophys. Acta* **2008**, *1780*, 325–346. [[CrossRef](#)] [[PubMed](#)]
13. Henderson, J.K.; Draper, J.S.; Baillie, H.S.; Fishel, S.; Thomson, J.A.; Moore, H.; Andrews, P.W. Preimplantation human embryos and embryonic stem cells show comparable expression of stage-specific embryonic antigens. *Stem Cells* **2002**, *20*, 329–337. [[CrossRef](#)] [[PubMed](#)]
14. Takahashi, K.; Tanabe, K.; Ohnuki, M.; Narita, M.; Ichisaka, T.; Tomoda, K.; Yamanaka, S. Induction of pluripotent stem cells from adult human fibroblasts by defined factors. *Cell* **2007**, *131*, 861–872. [[CrossRef](#)] [[PubMed](#)]
15. Brimble, S.N.; Sherrer, E.S.; Uhl, E.W.; Wang, E.; Kelly, S.; Merrill, A.H., Jr.; Robins, A.J.; Schulz, T.C. The cell surface glycosphingolipids SSEA-3 and SSEA-4 are not essential for human ESC pluripotency. *Stem Cells* **2007**, *25*, 54–62. [[CrossRef](#)] [[PubMed](#)]
16. Slambrouck, S.V.; Steelant, F.A. Clustering of monosialyl-Gb5 initiates downstream signaling events leading to invasion of MCF-7 breast cancer cells. *Biochem. J.* **2007**, *401*, 689–699. [[CrossRef](#)]
17. Saito, S.; Orikasa, S.; Satoh, M.; Ohyama, C.; Ito, A.; Takahashi, T. Expression of globo-series gangliosides in human renal cell carcinoma. *Jpn. J. Cancer Res.* **1997**, *88*, 652–659. [[CrossRef](#)]

18. Charafe-Jauffret, E.; Ginestier, C.; Iovino, F.; Wicinski, J.; Cervera, N.; Finetti, P.; Hur, M.H.; Diebel, M.E.; Monville, F.; Dutcher, J.; et al. Breast cancer cell lines contain functional cancer stem cells with metastatic capacity and a distinct molecular signature. *Cancer Res.* **2009**, *69*, 1302–1313. [[CrossRef](#)]
19. Hung, T.-C.; Lin, C.-W.; Hsu, T.-L.; Wu, C.-Y.; Wong, C.-W. Investigation of SSEA-4 binding protein in breast cancer cells. *J. Am. Chem. Soc.* **2013**, *135*, 5934–5937. [[CrossRef](#)]
20. Bremer, E.G.; Levery, S.B.; Sonnino, S.; Ghidoni, R.; Canevari, S.; Kannagi, R.; Hakomori, S. Characterization of a glycosphingolipid antigen defined by the monoclonal antibody MBr1 expressed in normal and neoplastic epithelial cells of human mammary gland. *J. Biol. Chem.* **1984**, *259*, 14773–14777.
21. Sato, B.; Katagiri, Y.U.; Miyado, K.; Akutsu, H.; Miyagawa, Y.; Horiuchi, Y.; Nakajima, H.; Okita, H.; Umezawa, A.; Hata, J.; et al. Preferential localization of SSEA-4 in interfaces between blastomeres of mouse preimplantation embryos. *Biochem. Biophys. Res. Commun.* **2007**, *364*, 838–843. [[CrossRef](#)]
22. Steelant, W.F.; Kawakami, Y.; Ito, A.; Hanada, K.; Bruyneel, E.A.; Mareel, M.; Hakomori, S. Monosialyl-Gb5 organized with cSrc and FAK in GEM of human breast carcinoma MCF-7 cells defines their invasive properties. *FEBS Lett.* **2002**, *531*, 93–98. [[CrossRef](#)]
23. Nunomura, S.; Ogawa, T. A total synthesis of a stage specific embryonic antigen-3 (SSEA-3), globopentaosyl ceramide, IV3GalGb4Cer. Use of 2,4,6-trimethylbenzoyl group as a stereocontrolling auxiliary. *Tetrahedron Lett.* **1988**, *29*, 5681–5684. [[CrossRef](#)]
24. Park, T.K.; Kim, I.J.; Danishefsky, S.J. A total synthesis of a stage specific pentasaccharide embryogenesis marker. *Tetrahedron Lett.* **1995**, *36*, 9089–9092. [[CrossRef](#)]
25. Ishida, H.; Miyawaki, R.; Kiso, M.; Hasegawa, A. Synthetic studies on sialoglycoconjugates 82: First total synthesis of sialyl globopentaosyl ceramide (V<sup>3</sup>Neu5AcGb<sub>5</sub>Cer) and its positional isomer (V<sup>6</sup>Neu5AcGb<sub>5</sub>Cer). *J. Carbohydr. Chem.* **1996**, *15*, 163–182. [[CrossRef](#)]
26. Lassaletta, J.M.; Schmidt, R.R. Versatile approach to the synthesis of globoside glycosphingolipids synthesis of sialyl-galactosyl-globoside. *Tetrahedron Lett.* **1995**, *36*, 4209–4212. [[CrossRef](#)]
27. Bilodeau, M.T.; Park, T.K.; Hu, S.; Randolph, J.T.; Danishefsky, S.J.; Livingston, P.O.; Zhang, S. Total synthesis of a human breast tumor associated antigen. *J. Am. Chem. Soc.* **1995**, *117*, 7840–7841. [[CrossRef](#)]
28. Imamura, A.; Ando, H.; Ishida, H.; Kiso, M. Ganglioside GQ1b: Efficient total synthesis and the expansion to synthetic derivatives to elucidate its biological roles. *J. Org. Chem.* **2009**, *74*, 3009–3023. [[CrossRef](#)]
29. Imamura, A.; Ando, H.; Korogi, S.; Tanabe, G.; Muraoka, O.; Ishida, H.; Kiso, M. Di-*tert*-butylsilylene (DTBS) group-directed  $\alpha$ -selective galactosylation unaffected by C-2 participating functionalities. *Tetrahedron Lett.* **2003**, *44*, 6725–6728. [[CrossRef](#)]
30. Imamura, A.; Matsuzawa, N.; Sakai, S.; Udagawa, T.; Nakashima, S.; Ando, H.; Ishida, H.; Kiso, M. The origin of high stereoselectivity in di-*tert*-butylsilylene-directed  $\alpha$ -galactosylation. *J. Org. Chem.* **2016**, *81*, 9086–9104. [[CrossRef](#)]
31. Asano, S.; Tanaka, H.-N.; Imamura, A.; Ishida, H.; Ando, H. *p-tert*-Butyl groups improve the utility of aromatic protective groups in carbohydrate synthesis. *Org. Lett.* **2019**, *21*, 4197–4200. [[CrossRef](#)]
32. Furusawa, K. Removal of cyclic di-*t*-butylsilylanediyl protecting groups using tributylamine hydrofluoride (TBAHF) reagent. *Chem. Lett.* **1989**, *18*, 509–510. [[CrossRef](#)]
33. Yu, B.; Tao, H. Glycosyl trifluoroacetimidates. Part 1: Preparation and application as new glycosyl donors. *Tetrahedron Lett.* **2001**, *42*, 2405–2407. [[CrossRef](#)]
34. Komura, N.; Kato, K.; Udagawa, T.; Asano, S.; Tanaka, H.-N.; Imamura, A.; Ishida, H.; Kiso, M.; Ando, H. Constrained sialic acid donors enable selective synthesis of  $\alpha$ -glycosides. *Science* **2019**, *364*, 677–680. [[CrossRef](#)] [[PubMed](#)]
35. Tanaka, H.; Ando, H.; Ishihara, H.; Koketsu, M. Sialylation reactions with 5-*N*,7-*O*-carbonyl-protected sialyl donors: Unusual stereoselectivity with nitrile solvent assistance. *Carbohydr. Res.* **2008**, *343*, 1585–1593. [[CrossRef](#)]
36. Sugimura, T.; Hagiya, K. Di-2-methoxyethyl azodicarboxylate (DMEAD): An inexpensive and separation-friendly alternative reagent for the Mitsunobu reaction. *Chem. Lett.* **2007**, *36*, 566–567. [[CrossRef](#)]
37. Hagiya, K.; Muramoto, N.; Misaki, T.; Sugimura, T. DMEAD: A new dialkyl azodicarboxylate for the Mitsunobu reaction. *Tetrahedron* **2009**, *65*, 6109–6114. [[CrossRef](#)]
38. Tamai, H.; Ando, H.; Tanaka, H.-N.; Hosoda-Yabe, R.; Yabe, T.; Ishida, H.; Kiso, M. The total synthesis of the neurogenic ganglioside LLG-3 isolated from the Starfish *Linckia laevigata*. *Angew. Chem. Int. Ed.* **2011**, *50*, 2330–2333. [[CrossRef](#)]

39. Ishiwata, A.; Munemura, Y.; Ito, Y. Synergistic solvent effect in 1,2-*cis*-glycoside formation. *Tetrahedron* **2008**, *64*, 92–102. [[CrossRef](#)]
40. Mandal, S.S.; Liao, G.; Guo, Z. Chemical synthesis of the tumor-associated Globo-H antigen. *RSC Adv.* **2015**, *5*, 23311–23319. [[CrossRef](#)]
41. Kenworthy, A.K.; Nichols, B.J.; Remmert, C.L.; Hendrix, G.M.; Kumar, M.; Zimmerberg, J.; Lippincott-Schwartz, J. Dynamics of putative raft-associated proteins at the cell surface. *J. Cell Biol.* **2004**, *165*, 735–746. [[CrossRef](#)]
42. Lingwood, D.; Ries, J.; Schwille, P.; Simons, K. Plasma membranes are poised for activation of raft phase coalescence at physiological temperature. *Proc. Natl. Acad. Sci. USA* **2008**, *105*, 10005–10010. [[CrossRef](#)] [[PubMed](#)]
43. Baumgart, T.; Hammond, A.T.; Sengupta, P.; Hess, S.T.; Holowka, D.A.; Baird, B.A.; Webb, W.W. Large-scale fluid/fluid phase separation of proteins and lipids in giant plasma membrane vesicles. *Proc. Natl. Acad. Sci. USA* **2007**, *104*, 3165–3170. [[CrossRef](#)] [[PubMed](#)]
44. Levental, I.; Grzybek, M.; Simons, K. Raft domains of variable properties and compositions in plasma membrane vesicles. *Proc. Natl. Acad. Sci. USA* **2011**, *108*, 11411–11416. [[CrossRef](#)] [[PubMed](#)]



© 2019 by the authors. Licensee MDPI, Basel, Switzerland. This article is an open access article distributed under the terms and conditions of the Creative Commons Attribution (CC BY) license (<http://creativecommons.org/licenses/by/4.0/>).